# Energy Band Diagram of NiO: Lu$_2$O$_3$/n-Si heterojunction

## Isam M. Ibrahim[1], Abubaker S. Mohammed[2]*, Asmiet Ramizy[2]

[1]Department of Physics, College of Science, University of Baghdad, Baghdad, Iraq.
[2]Department of Physics, College of Science, University of Anbar, Anbar, Iraq.

**Abstract**

Crystalline NiO and doped with rare earth lutetium oxide (Lu$_2$O$_3$) at (6%wt)., have been prepared by pulsed laser deposition (PLD), The Q-switched Nd:YAG laser beam was incident at an angle of 45° on the target surface, and the energy of the laser was 500 mJ, wavelengths of 532nm, and frequency 6Hz. XRD pattern shows all doped and undoped films are polycrystalline, and cubic structure. The 200nm thin NiO showed an average optical energy band gap of 3.4eV, and increase with doping at 6% Lu$_2$O$_3$. The Hall Effect measurements confirmed that holes were predominant charges in the conduction process (i.e p-type). D.C conductivity measurements with temp-erature (T), show that the films prepared have the two activation energy increase with doping of Lu$_2$O$_3$. Capacitance-voltage (C-V) measurements were performed for films prepared, where the built in voltage has been determined and decreases in value when doping with the rare earth. In this study we assumed an energy band diagram for p-NiO /n-Si heterojunction.

**Key words:** Thin film of NiO, Rare Earth, PLD, Energy Band diagram.

## مخطط حزم الطاقة للمفرق المتباين NiO: Lu$_2$O$_3$/Si

### عصام محمد أبراهيم[1]، أبوبكر صبار محمد[2]*، عصمت رمزي[2]

[1]قسم الفيزياء، كلية العلوم، جامعة بغداد، بغداد، العراق.
[2]قسم الفيزياء، كلية العلوم، جامعةالأنبار، الأنبار، العراق.

**الخلاصة**

تم تحضير أغشية أوكسيد النيكل البلوري المطعم بعنصر الليتتيوم النادر عند نسبة 6% بواسطة الترسيب بالليزر النبضي. وكان شعاع الليزر نيدميوم–ياك يسقط عند زاوية 45 درجة على سطح الهدف، طاقة ليزر 500mJ، طول موجي 532nm, وتردد 6Hz. أنماط حيود الاشعة السينية بينت ان الأغشية المحضرة النقية والمطعمة متعددة التبلور وذات تركيب بلوري مكعبي. غشاء اوكسيد النيكل الرقيق ذا سمك 200 نانومتر يمتلك فجوة طاقة بصرية مقدارها 3.4 الكترون–فولت وتزداد قيمتها عند التطعيم بالعنصر Lu$_2$O$_3$ عند نسبة 6%. اكدت قياسات تأثير هول ان الفجوات هي الشحنات السائدة في عملية التوصيل اي انه موجب الشحنة. وضحت قياسات التوصيلية المستمرة ان الاغشية المحضرة تمتلك طاقتي تنشيط تزداد قيمتها عند التطعيم بالليتتيوم. تم اجراء قياسات سعة–جهد حيث تم تحديد جهد البناء الداخلي والذي تنخفض قيمته عند التطعيم بالعنصر النادر .في هذه الدراسة نفترض مخطط حزم الطاقة للمفرق المتباين p–NiO/n–S .

---

*Email: baker.sabbar3@gmail.com

## 1. Introduction

Nickel oxide (NiO) is one of material considered to be a model p-type semiconductor with having a wide band-gap energy about 3.6 eV to 4.0 eV[1]. NiO show attractive material because high chemical stability, low cost, promising ion storage material in terms of high stability and it is have a wide range of applications[2, 3]. NiO is a promising candidate for UV photodetectors as well as for organic and inorganic solar cells, and thin film transistors[4-7]. The color of NiO very sensitive to the presence of higher valence states of Ni even in traces, also non-stoichiometric of NiO result from the presence of nickel positive vacancy and interstitial molecules oxygen in NiO crystalline lattice [8]. The green color is commonly for NiO stoichiometric semiconductors [9].The NiO thin films have been prepared by different techniques including, pulsed laser deposition(PLD), spray pyrolysis, sputtering, sol-gel, and thermal evaporation[10-14]. Nowadays the PLD is a one of important method used to synthesis high-quality thin films that is advantageous in tuning the matter characteristics .where, there are a few reports on the fabrication of NiO thin film via PLD [15]. Rare Earth (RE) element are a group of 17 element[16] such as cerium, lanthanum ,lutetium, etc., Lutetium oxide ($Lu_2O_3$) is a very attractive host material for different application due to its wide band gap and convenient properties such as (phase stability, chemical stability and low thermal expansion).[17] The RE doped with metal-oxide-semiconductor (MOS) such as NiO, appeared high matching with standard completely metal oxide semiconductor (CMOS) processes combined with the excellent optical properties of rare earth elements[18]. The aim of the present work is to pay more attention to study of the junction of p-$NiO:Lu_2O_3$/n-Si heterojunction and effect of rare earth on the structural, optical and electrical behavior on nickel oxide thin films prepared by pulsed laser deposition

## 2. Experimental Setup

Thin NiO films were deposited on glass and silicon (n-type (111 orientation), using PLD technique. NiO powders doping with 6% ($Lu_2O_3$) were mixed using a gate mortar and then pressed under 5ton to form targets with 2cm diameter and 0.2 cm thickness. The target were ensured to be dense and homogeneous as possible to produce good quality $NiO:Lu_2O_3$ billet, which would be deposited by the PLD technique. Film deposition was carried out inside a $10^{-3}$ Torr evacuated chamber. Si wafer was cut into square-shape pieces ($1cm^2$) and the Si wafers were ultrasonically cleaned in distilled water and acetone. The film thickness was determined by Filmetrics (F20) and varied within $200 \pm 5$ nm. The structure of the films were examined by X-raydiffraction (XRD-6000-shemadzu with CuKα, wavelength =1.54 A$^{°}$). The hetrojunction was fabricated by the metallization of samples, and the metal contacts of finger-shaped gold (Au) electrodes of 200 nm thickness were deposited on top of the $NiO:Lu_2O_3$/n-Si sample using an E306A Edwards thermal evaporation system. The UV-Visible optical transmission spectra of the thin films were recorded by (Shemadzu UV-160/UV-Visible recorder spectrophotometer). Hall effect, Dc electrical conductivity, were measured to determine the type of NiO film and the electrical conductivity (Digital electrometer type Ketheley 616 was used for this purpose). The C-V characteristic were carried out (using LCR meter model HP-R2CC4274).

## 3. Result and Discussion

### 3.1 Structure

Figure-1 shows the XRD pattern of NiO thin film doped with rare earth $Lu_2O_3$ deposited on n-Si at room temperature substrate temperature. XRD pattern shows that all doped and undoped films are polycrystalline. The XRD pattern exhibits numerous peaks at 2θ of 37.3 and 43.3, which are referred to (111) and (200) planes of the cubic structure of NiO, respectively, according to the JCPDS file (card no.96-900-8694). This result is in agreement with that of Sta [19]. many peaks referring to lutetium oxide at 2θ of 29.8, 34.5, and 49.6 are observed and refer to the (222), (400), and (440) planes of the cubic structure of $Lu_2O_3$, respectively, from the International Center for Diffraction (card no. 96-101-0596). Table-1 shows the experimental data of standard peaks. The result shows that the mean crystallite size of NiO films decreases with doping, and FWHM both increases, as shown in Table-1. This result indicates that the nano crystalline are domains.
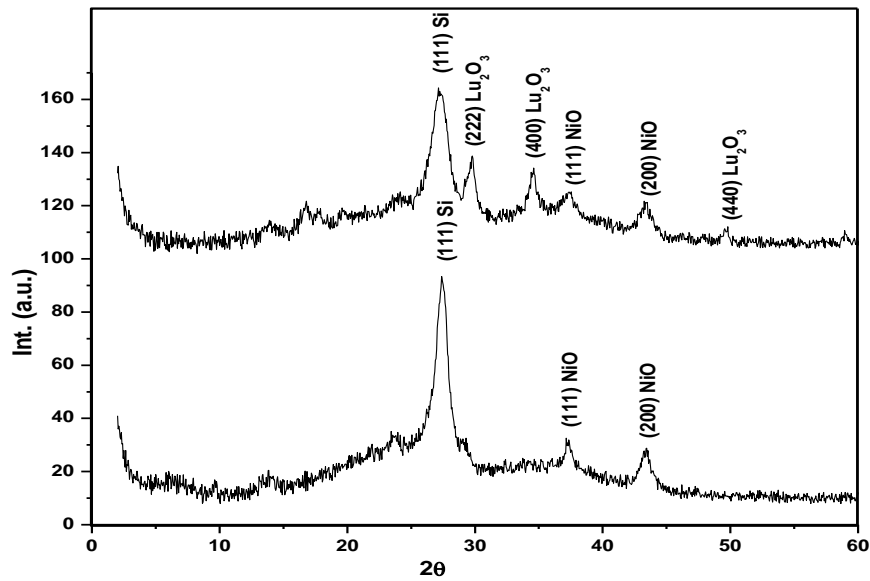
**Figure 1**-X-ray diffraction patterns of $Lu_2O_3$-doped NiO /n-Si doping ratios of 0, and 6% wt.

**Table1-**Structural parameters of $Lu_2O_3$-doped NiO/n-Si deposited at different doping ratios 0 and 6 %wt.

| $Lu_2O_3$% | 2θ (Deg.) | FWHM (Deg.) | $d_{hkl}$ | G.S (nm) | $d_{hkl}$ Std.(Å) | hkl | phase | Card No. |
|---|---|---|---|---|---|---|---|---|
| **0** | 27.4520 | 0.8818 | 3.2464 | 9.3 | (111) | 3.1414 | Cub. Si | 96-901-3105 |
| | 37.3200 | 0.6446 | 2.4076 | 13.0 | (111) | 2.4066 | Cub. NiO | 96-900-8694 |
| | 43.3800 | 0.9829 | 2.0842 | 8.7 | (200) | 2.0842 | Cub. NiO | 96-900-8694 |
| **6** | 27.3310 | 1.3030 | 3.2605 | 6.3 | (111) | 3.1414 | Cub. Si | 96-901-3105 |
| | 29.8011 | 0.6540 | 2.9956 | 12.6 | (222) | 2.9936 | Cub.$Lu_2O_3$ | 96-101-0596 |
| | 34.5410 | 0.7150 | 2.5946 | 11.6 | (400) | 2.5925 | Cub.$Lu_2O_3$ | 96-101-0596 |
| | 37.3520 | 1.1160 | 2.4056 | 7.5 | (111) | 2.4066 | Cub. NiO | 96-900-8694 |
| | 43.3260 | 1.1180 | 2.0867 | 7.6 | (200) | 2.0842 | Cub. NiO | 96-900-8694 |
| | 49.6660 | 0.5420 | 1.8342 | 16.2 | (440) | 1.8332 | Cub.$Lu_2O_3$ | 96-101-0596 |

## 3.2 Optical properties

   Optical energy gap can be used to estimate the difference in energy between the valence and conduction bands, which can help determine the thermoelectric and electronic properties of the materials. The direct energy gap Eg is determined by using Tauc formula, with relation r = 1/2 yields linear dependence. The optical band gap of NiO films of undoped and doped lutetium is shown in Figure-2 from the plot of $(\alpha h\nu)^2$ as a function of photon energy (hν). From Figure-2, the energy band gap of NiO at a thickness of 200 nm is found to be notably 3.4 eV. The NiO doping with 6% lutetium increases the band gap energy to 3.8 eV as in Table-2. This trend shifted toward high energy (blue shift) as a result of the reduction of grain size [20]. This result can be attributed to the quantum confinement effects which specifically occur in semiconductor nanoparticles. The small size of nanoparticles is responsible for different properties, such as optical, electronic, and electrical [21]. The effect of quantum confinement leads to the increase of the energy band whenever the particle size decreases due to the restriction of particle movement in one dimension.
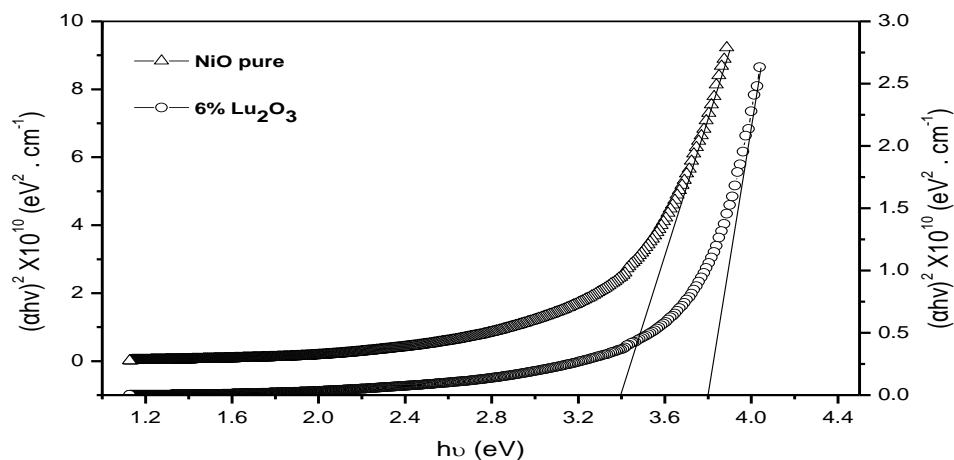
**Figure 2**-Optical energy gap of $Lu_2O_3$-doped NiO/n-Si at 0, and 6% wt.

**Table 2-** The activation energy, difference in valence and conduction band, optical energy gap.

| Sample | $Ea_1(eV)$ | $Ea_2(eV)$ | $\Delta E_v(eV)$ | $\Delta E_c(eV)$ | $Vbi(eV)$ | $Eg(eV)$ |
|---|---|---|---|---|---|---|
| pure NiO | 0.059 | 0.41 | - | - | 1.5 | 3.4 |
| 6% Lu | 0.101 | 0.58 | 0.15 | 2.53 | 1.1 | 3.8 |

### 3.3 Electrical properties

P-type conductivity have been estimated from Hall measurements for pure NiO films and doped with $Lu_2O_3$ which were deposited on glass substrates.

The electrical properties of D.C conductivity measurements ($\sigma_{d.c}$) with temperature (T) and the activation energy of undoped and doped films illustrate in Figure-3. This figure show the linear relationship between Ln $\sigma$ and 1000/T, which is used to calculate the activation energy ($E_a$).The change in the conductivity mechanism, due to the existence of two connecting regions. The first region is at low temperature (373K°) which is the carrier transport between inside optical energy gap. The second region is at temperatures higher than 373K°[22]. Table-2 show the two activation energy increase with doping, the increasing in activation energy with doping may be return to increasing in energy gap.
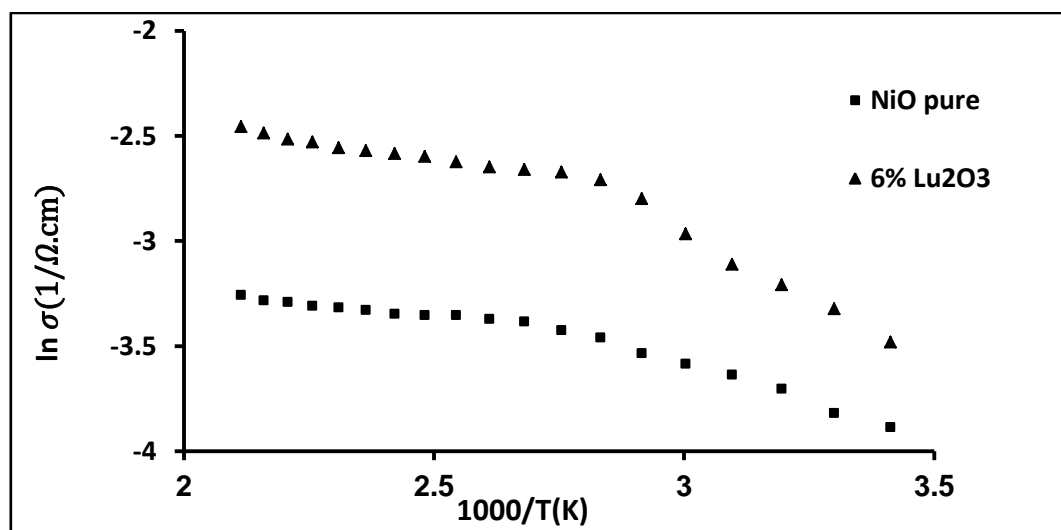


**Figure 3-** Variation of Ln ($\sigma$) with reciprocal temperature for $Lu_2O_3$-doped NiO at 0, and 6 %wt.

### 3.4 C-V characteristics

The variation of capacitance as a function of forward and reverse bias voltage in the range of (0-1)V at frequency equal to 100 kHz has been studied, for NiO/n-Si heterojunction for as deposited and effect of rare earth. The linear relationship between the voltage and the inverted square capacitance is illustrated in Figure-4. The plots revealed straight line relationship which means that the junction was of an abrupt type. The interception of the straight line with the voltage axis at $(1/C^2) = 0$ represents the built-in voltage($V_{bi}$). Table-2 show the decrease in $V_{bi}$ with add $Lu_2O_3$ doping.
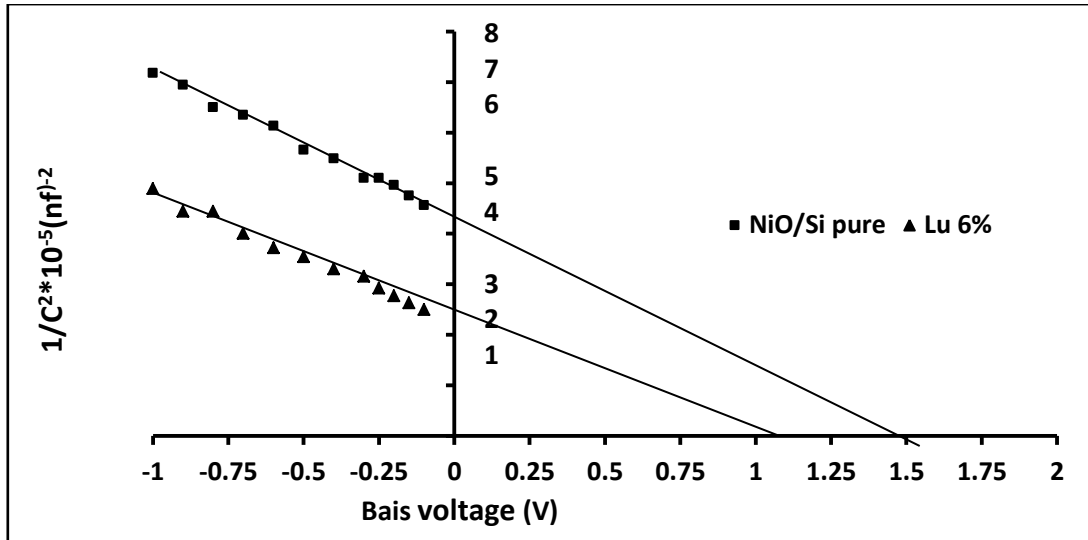


**Figure 4-** Internal built voltage of $Lu_2O_3$-doped NiO at (0, and 6)%wt.

### 3.5 Energy Band Diagram

Energy band diagram for NiO: $Lu_2O_3$/n-Si at 6% heterojunction have been introduced as shown in Figure-5. With aid of optical energy gap, dc-conductivity, and C-V measurement. At a hetrojunction each of semiconductor may be doped p-type or n-type, so there are four combinations, namely p-P, n-N (isotype) and P-n, N-p (anisotype) junction, the capital latter refer to the wider band gap[23].without any external bias the p-NiO contacts with n-Si the holes will diffuse from p-NiO to n-Si, As a result these diffuse the negative space charge will remain in the p-NiO near the junction, and so that the band bend downwards in NiO, the band bends in n-Si upward result from decrease in the valence band energy. According to Anderson model the change in conduction band is equal $\Delta E_c$, and the valence band offset $\Delta E_v$ showed in Figure-2. All parameters in order to plot the energy band diagram are $\mathbf{\Delta Ec}$ and $\Delta Ev$ which can be calculated from equation (1 to 2) [24].

$$\Delta Ec = \chi_n - \chi_p \dots\dots\dots\dots\dots\dots\dots\dots\dots\dots\dots\dots\dots\dots\dots\dots\dots\dots\dots\dots\dots\dots\dots (1)$$

$$\Delta E_v = \left(Eg_p - Eg_n\right) - (\chi_n - \chi_p) \quad \dots\dots\dots\dots\dots\dots\dots\dots\dots\dots\dots\dots\dots\dots\dots (2)$$

Where $Eg_p$, $Eg_n$ is optical energy gap for p and n-type semiconductors, $E_{an}$, $E_{ap}$ is activation energy for n and p-type semiconductor. This energy band profile in which a "spike" and "notch" occur in the conduction band edges at the interface is the case in which $\chi_n > \chi_p$. Experimentally it is found the two semiconductors have different electron affinity ($\chi$), different energy gaps ($E_g$), different work function ($\phi$) and different dielectric constants($\varepsilon$).
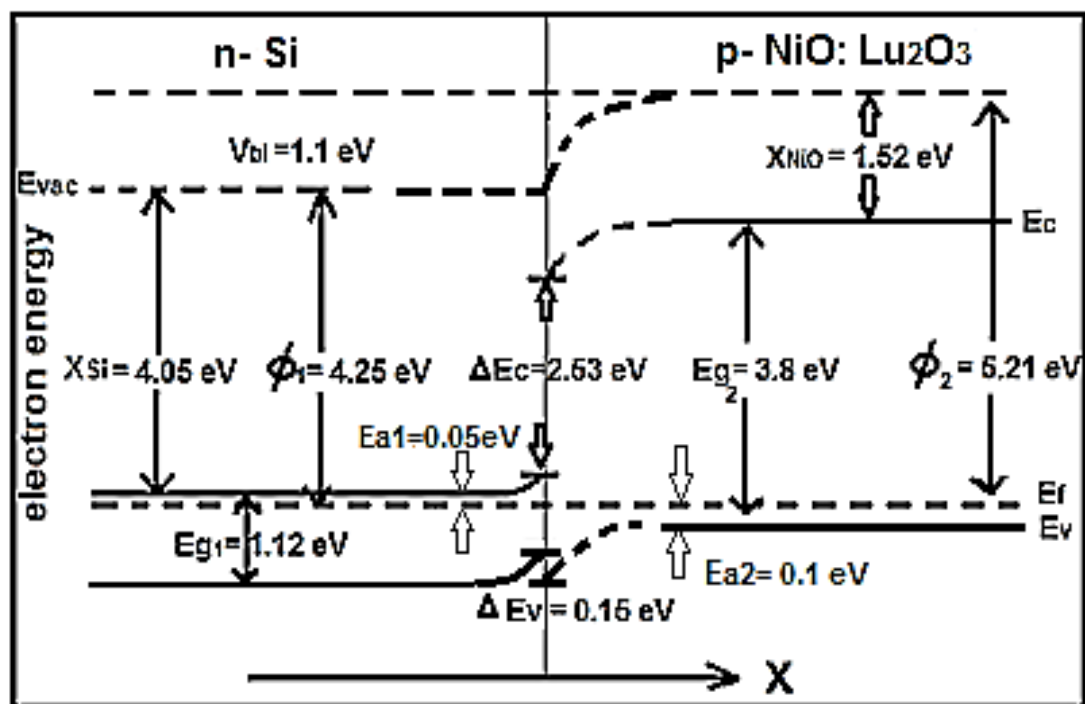
**Figure 5-** Energy band diagram of p-NiO/n-Si Hetrojunction doped with $Lu_2O_3$ at 6 % wt.

## 4. Conclusion

Nickel oxide doped with rare earth deposited on silicon substrate by pulsed laser prepared successfully. XRD pattern of films show that the doping leads to broadening in diffraction peaks. The optical energy gap increase at doping with $Lu_2O_3$ at 6%wt. Energy band diagram model for our result has been presented to show the mechanism of electron transition within the junction.

## References

1. Stamataki, M., Tsamakis, D., Brilis, N., Fasaki, I., Giannoudakos, A. and Kompitsas, M. **2008**. Hydrogen gas sensors based on PLD grown NiO thin film structures. *phys. stat. sol.* (a), **205**(8): 2064–2068.
2. Jbaier, D.S., Simon, J.A., Khashan, K.S. **2015**. Nanostructure NiO films prepared by PLD and their optoelectronic properties. *Eng. &Tech. J.*, **33**(5): 951-959.
3. Saleh, A.F. **2013**. Structural and morphological studies of NiO thin films prepared by Rapid thermal oxidation method. *IJAIEM*, **2**(1): 16-21.
4. Zhang, D., Nozaki, S., Uchida, K. **2014.** NiO/Si heterostructures formed by UV oxidation of nickel deposited on Si substrates. *J. Vac. Sci. Technol*. B, **32**(3).
5. Shan, F., Liu, A., Zhu, H., Kong, W., Liu, J., Shin, B., Fortunato, E., Martins, R., Liu, G. **2016**. High-mobility p-type NiOx thin-film transistors processed at low temperatures with $Al_2O_3$ high-k dielectric. *J. Mater. Chem*. C4, **4**(40): 9439–9444.
6. Jung, J., Kim, D.L., Oh, S.H., Kim, H.J. **2012**. Stability enhancement of organic solar cells with solution-processed nickel oxide thin films as hole transport layer. *Sol. Energy Mater. Sol. Cells.*, **102**: 103–108.
7. Patel, D.B., Kim, H.S., Patel, M., Chauhan, K.R., Park, J.E., Lim, D., Kim, J. **2016.** Front surface field formation for majority carriers by functional p-NiO layer employed Si solar cell. *Appl. Phys. Lett.*, **109**(13): 29-34.
8. Subramanian, B., Mohamed Ibrahim, M., Senthilkumar, V., Murali, K.R., Vidhya, VS., Sanjeeviraja, C., Jayachandran, M**. 2008.** Optoelectronic and electrochemical properties of nickel oxide (NiO) films deposited by DC reactive magnetron sputtering. *Physica* B, **403**: 4104–4110.
9. Lu, Y.M., Hwang, W.S. and Yang, J.S. **2002.** Effects of substrate temperature on the resistivity of non-stoichiometric sputtered NiO films. *Surface and Coatings Technology*, **155**: 231-235.
10. Tareq, H.S. **2014.** Study the Effect of Rapid Thermal Annealing on Thin Films Prepared by Pulse Laser Deposition Method. *Eng. &Tech. J.*, **32**(3): 444-451.

11. Abdnabi, M., Aziz, K., Tarq, Z. **2014.** Optical and Structural Properties of NiO Thin Films Prepared by Spray Pyrolysis. Indian. *J. of Appl. research*. **4**(10): 533-537.
12. Vendano, E.A., Berggren, L., Niklasson, G.A., Granqvist, C.G. and Azens, A. **2006.** Electrochromic materials and devices: Brief survey and new data on optical absorption in tungsten oxide and nickel oxide films. *Thin Solid Films*., **496**(1): 30-36.
13. Alagiri, M., Ponnusamy, S., Muthamizhchelvan, C. **2012.** Synthesis and characterization of NiO nanoparticles by sol–gel method. *J Mater Sci: Mater Electron*., **23**(3): 728–732.
14. Choi, J.M., Im, S. **2005.** Ultraviolet enhanced Si-photodetector using p-NiO films., *Appl.Surf. Sci*., **244**(1-4): 435–438.
15. Jahromi, S.P., Huang, N.M., Kamalianfar, A., Lim, H.N., Muhamad, M.R. and Yousefi, R. **2012.** Facile Synthesis of Porous-Structured Nickel Oxide Thin Film by Pulsed Laser Deposition. *J. of Nanomaterials*, 2012, 1-4.
16. Zepf, V. **2013.** *Rare Earth Elements: What and Where They Are in Rare Earth Elements*, Chapter 2 , springer Link.,11–39.
17. An, L., Ito, A. and Goto, T. **2011**. Fabrication of Transparent Lutetium Oxide by Spark Plasma Sintering. *J. Am. Ceram. Soc*., **94**(3): 695–698.
18. Rebohle, L., Berencén, Y., Braun, M., Garrido, B., Hiller, D., Liu, B., Ramírez, J. M., Sun, J.M., Wutzler, R., Helm, M. and Skorupa, W. **2014.** Rare Earth Doped Metal-Oxide-Semiconductor Structures: A Promising Material System or a Dead End of Optoelectronic Evolution. *ECS Transactions*, **61**(5): 175-185.
19. Sta, M., Jlassi, M., Kandyla, M., Hajji, P., Koralli, R., Allagui, M., Kompitsas, and H. Ezzaouia, H. **2016.** Hydrogen sensing by sol-gel grown NiO and NiO:Li thin films. *J. of Alloys and Compounds*., **626**(87): 87-92.
20. Karpinski, A., Ouldhamadouche, N., Ferrec, A., Cattin, L., Richard-Plouet, M., Brohan, L., Djouadi, M.A., Jouan, P.Y**. 2011**. Optical characterization of transparent nickel oxide films deposited by DC current reactive sputtering. *Thin Solid Films*., **519**(17): 5767-5770.
21. Kruis, F.E., Fissan, H. and Peled, A. **1998.** Synthesis Of nanoparticles in the gas phase for electronic, optical and magnetic application –Areview. *J. Aerosol Sci*., **29**(5/6): 511-535.
22. Garde, S.A. **2010.** LPG and NH3 Sensing Properties of $SnO_2$Thick Film Resistors Prepared by Screen Printing Technique. *Sensors & Transducers J*., **122**(11): 128-142.
23. Sze, S.M. and Kwok K. Ng **1981.** *Physics of Semiconductor Devices*. 3th Ed, Wiley and Sons.
24. Ali, I.M. **2011.** Energy band diagram of In2O3/ Si heterojunction. *Baghdad. Sci. J*., **8**(2): 581-586.